Marine and Petroleum Geology *[submitted]*

Contents lists available at ScienceDirect

Marine and Petroleum Geology

journal homepage: www.elsevier.com/locate/marpetgeo

Research Article

Empirical relationship between river slope and the elongation of bars in braided rivers: a potential tool for paleoslope analysis from subsurface data

Sébastien Castelltort [a,*]

[a] *Department of Earth Sciences, University of Geneva, Rue des Maraichers 13, 1205 Geneva, Switzerland*

Keywords
Braided river
Subsurface
Paleoslope
Seismic geomorphology
Reservoir properties
Fluvial systems
Sedimentation

A B S T R A C T

Paleoslope of ancient river systems is a fundamental parameter needed to reconstruct paleohydrology and paleoclimate from the fluvial sedimentary record. The shape of braid bars in 22 modern rivers yields a relationship between average bar elongation (length/width) and river slope. Steep rivers display more elongated bars than gently dipping reaches. This relationship has potential application to ancient braided systems preserved in the subsurface and imaged by 3D seismic data. The average elongation of bars identified on a stratal-slice through the DaGang river deposits in North-East China yields a slope prediction which, combined with empirical data on grain size and slope of alluvial rivers, predicts a median grain size of between 0.1 and 1 mm for the considered river sediment, in agreement with grain size data in an adjacent isochronous belt. This study provides an additional approach for paleohydraulics in sedimentary basins and grain size prediction in exploration.

1. Introduction

Paleoslope is a parameter of fundamental importance for reconstructing paleohydrology, paleoclimate and tectonics from the fluvial archives (Paola and Mohrig, 1996, Duller et al., 2012), understand the controls on aggradation, degradation and signal transmission in fluvial systems (Castelltort and Van Den Driessche, 2003, Romans et al., 2016), and predict grain size and reservoir properties in hydrocarbon exploration and water resource management (e.g., Bhattacharya and Tye, 2004). Braided rivers consist of multiple channels characterized by fundamental morphological units made of channel confluences-bifurcations separating pool-bars visible at median and low water stage (Ferguson, 1993, Ethridge and Schumm, 2007, Hundey and Ashmore, 2009). Although there seems to be generally

* Corresponding author. Tel: +41 223796616
E-mail address: sebastien.castelltort@unige.ch (S. Castelltort)

accepted single mode of braid development (Ferguson, 1993), observations of case studies, physical experiments (Ashmore, 1982, Ashmore, 1991, Leopold and Wolman, 1957) and numerical models (Murray and Paola, 1994, review in Williams et al., 2016) converge towards emphasizing the importance of excess bedload deposition at flow bifurcations, due to loss of transport capacity, and scour at convergences when flow regains competence. In this context, although variations in discharge are not seen as a necessary condition for the formation of a braiding pattern (Leopold and Wolman, 1957, Ashmore, 1991, Germanoski and Schumm, 1993, Murray and Paola, 1994, Schuurman et al., 2013), processes of bar dissection at high-water stage and during flood recession have been proposed as playing an important, although debated, role among mechanisms of braid development (Ashmore, 1991, Ferguson, 1993, Knighton, 1998). Bar dissection induce the formation of divergent and convergent erosional networks (Lewin and Brewer, 2001) that modify primarily the sides and downstream ends of bars (Ferguson, 1993), but can also propagate upstream by headward erosion and connect with upstream channels, isolating new bar forms. Such erosional convergent networks in braided rivers are ubiquitous and particularly visible on aerial imagery (figure 1).

Several studies based on observation, physical and numerical experiments have demonstrated that the form of erosional fluvial networks is dependent, at their inception, on the slope of the surface on which water flows (Schumm, 1956, Schumm, 1977, Phillips and Schumm, 1987, Pelletier, 2003, Simpson and Schlunegger, 2003, Castelltort, et al., 2009, Jung et al., 2011, Castelltort and Yamato, 2013, McGuire et al., 2013). Depending on initial surface roughness (local relief prior to dissection), steep slopes tend to develop elongate and narrow drainage networks, i.e. with channels flowing rather parallel and converging at small angles, whereas gentle slopes produce more dilated and broader river basins with large channel convergence angles (Castelltort et al., 2009, Jung et al., 2011, Castelltort and Yamato, 2013, McGuire et al., 2013).

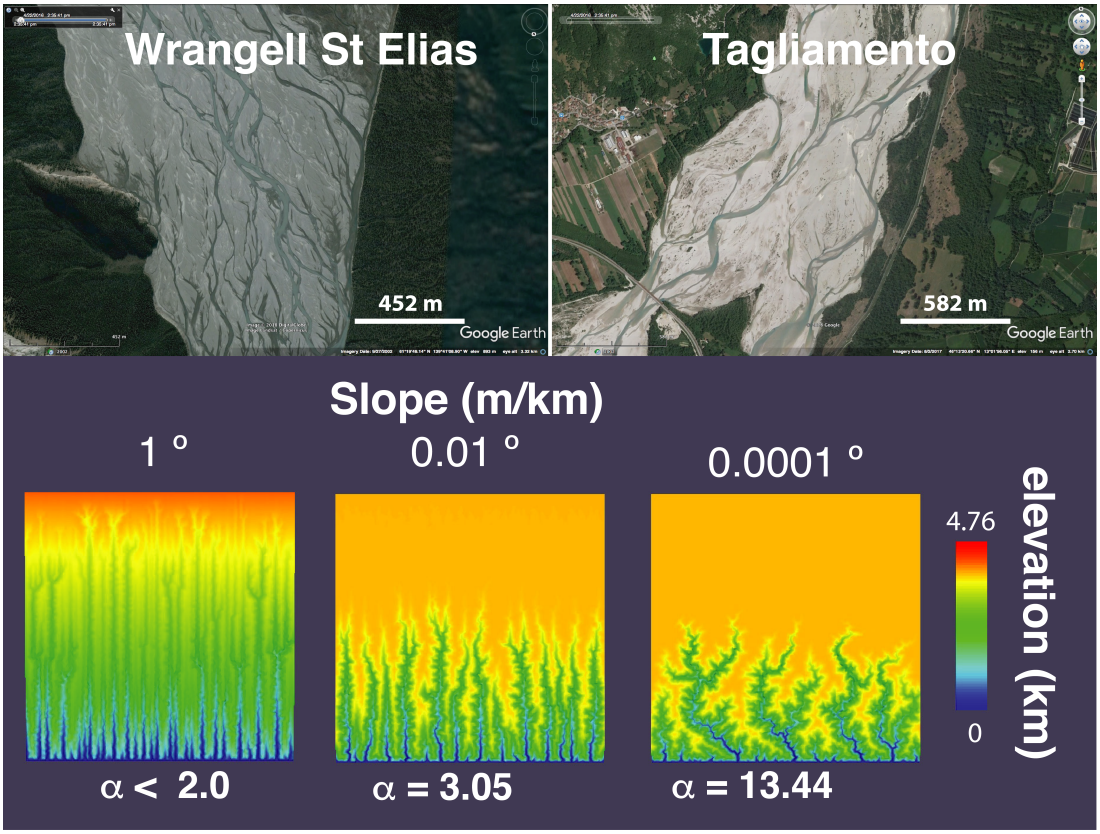

Figure 1 Braided rivers and dendritic drainage networks. Upper panel: both aerial views (Google Earth 2018, image Landsat / Copernicus) highlight the dendritic nature of the channel networks that dissect the active river bed and bars, visible at low stage. Flow is to the image bottom. Wrangell St Elias river image coordinates: 61°19'49.14"N / 139°41'8.90"W. Tagliamento river image coordinates: 46°13'20.85"N / 13° 1'54.33"E. Bottom panel: numerical

experiments of drainage network inception on undissected surfaces showing the effect of surface slope on channels convergence angles (α), modified from Castelltort and Yamato (2013). Based on the idea that channel networks dissecting fluvial bars in braided rivers contribute to their shaping to some extent, the objective of the present paper is to test whether the shape of bars exhibits a dependency on river slope.

These considerations emphasize that 1) bars in braided rivers can be formed and/or modified to some extent by convergent erosional networks linked to incision during overflow and flood recession, and 2) that the shape of incipient fluvial erosional networks in nature, numerical and physical experiments is to some extent dependent on surface slope. Thus, the question arises as to whether alluvial slope has an influence on the shape of braid bars through its influence on erosional networks. The ambition and scope of this paper is to provide an empirical view on this question, as a first step guiding future process-oriented research.

The approach followed is based on investigating braid bar geometry (defined by bar width and length or their ratio, bar elongation) because it is amenable to measurement and can be assumed as a reflecting channel network convergence pattern: elongated bars represent channel flowing parallel to each others, whereas broad and equant bars represent channels flowing and converging at large angle with each other. The convergence angle between individual channels in an alluvial braided river is indeed not practical to assess since it may be modified locally by channel bank collapse due to slope instability, erosive processes originating from excess bed scouring at the downstream confluence and lateral erosion due to channel lateral dynamics (Parker, 1978, Ashmore and Parker, 1983, Blondeaux and Seminara, 1985, Murray and Paola, 1994, Wheaton et al., 2013). Thus, in order to test the question formulated above, the present paper documents braid bar statistics from a set of braided rivers over a large range of slopes. To show the potential application of the relationship found between bar elongation and river slope, the paleoslope of a fossil braided river is evaluated from subsurface seismic data and discussed in terms of possible subsurface reservoir grain size predictions.

2. Material and Method

Braided rivers bar geometry data are extracted from GoogleEarth™ aerial images from the reaches (Table 1) of 22 rivers with constant slopes of between 0.8×10^{-3} and 17.2×10^{-3} over lengths of 2 to 200 km. The considered rivers are braided in the sense of "having a number of alluvial channels with bars and islands between meeting and dividing again" (Lane, 1957, cited in Sapozhnikov and Foufoula-Georgiou, 1996), generally originate from mountainous catchments and are generally devoid of bar top vegetation testifying of their active nature and of the submerged character of most bars at bankfull (hence prone to dissection). However, a minor amount of the braid bars and channels considered here (see Supplementary material) still show some degree of vegetation on bar tops, with possible stabilization and anabranching (e.g. Yukon, Amguema, Feshie). Other types of multiple-channel rivers such as large anabranching rivers (sometimes known as "mega complex anabranching rivers", e.g. the Negro or the Upper Congo rivers, Bristow and Best, 1993, Latrubesse, 2008) are examples showing extensive vegetation-mediated stabilization of banks that promote formation of fluvial archipelagos differing substantially from the braid bars studied here and for which mechanisms of bar dissection, bank and general processes of macroforms genesis are different from those active in the rivers considered in the present work. As in other studies of braid bar geometries (e.g., Sapozhnikov and Foufoula-Georgiou, 1996,, Walsh and Hicks, 2002, Kelly, 2006), the braid bars are digitized based on their individualization from other bars by visible channels, and there has been no attempt to perform measurements at different river stages to account for variations in bar exposure (see discussion in Kelly, 2006 and Egozi and Ashmore, 2008). The studied reaches have lengths that are more than 10 times the wetted width of the considered rivers, thus satisfying Egozi and Ashmore (2008)'s 20% precision criterion for braiding indices. Similarly to Kelly (2006), no attempt was made

to distinguish between simple and compound bars. Maps of bars contours are generated for each studied river segment and analyzed with the image components analysis tools of JMicroVision© (Roduit, accessed August 2017) to obtain the length (long axis) and width (widest part of the bar perpendicularly to the long axis) of all bars. Table 1 provides the name, coordinates, data source, and means of measured parameters of each studied river segment. A pdf file with assembled images and bar drawings for 16 of the rivers and kmz files of 6 rivers is available as supplementary data. Excepted for the Kosi (N=38) and Bléone (N=47) rivers, a minimum of 50 bars has been counted for each river (2120 bars in total). The typical vertical uncertainty of the SRTM elevation data used in GoogleEarth™ imagery is of a maximum of ±15 meters (Rodriguez, et al., 2005), which is taken into account for estimating maximum theoretical uncertainty on river slopes (given in Table 1).
Measured braid bar geometry is compared with Castelltort et al (2009)'s model for regional surface slope S_R control on drainage network convergence angle α, which is a measure of the width/length ratio of drainage basins, expressed as:

$$\alpha = 0.5\times \tan^{-1}(0.2067\times S_R^{-0.2342}) \qquad \text{equation 1}$$

Since elongation in the present work is the length/width ratio, predicted elongation E_p for each river considered here is computed simply by using river slope for S_R and taking the inverse of the tangent of equation 1.

3. Results

A total of 2120 bars were digitized and measured. The bars range in width from 3.6 m to 9.5 km and in length from 12 m to 23 km with large spread around these central values (see Supplementary table with descriptive statistics). Linear regression in logarithmic space of all bar length and width data yield the following scaling relationship for bar elongation (Fig 2A, blue regression line):

$$L = 4.53\times W^{0.9}, R^2 = 0.94 \qquad \text{equation 2}$$

Bar elongation (Fig 2B) defined as the bar length to bar width ratio is naturally less spread than width and length data (as a ratio of the two) and ranges from 1 to 7.6, with a mean of 3.1±1.08 (1 standard deviation) for all data. Within each river (see Supplementary table), elongations are normally distributed suggesting that the mean bar elongation can be used as an adequate descriptor of the shape of bars of a given river.

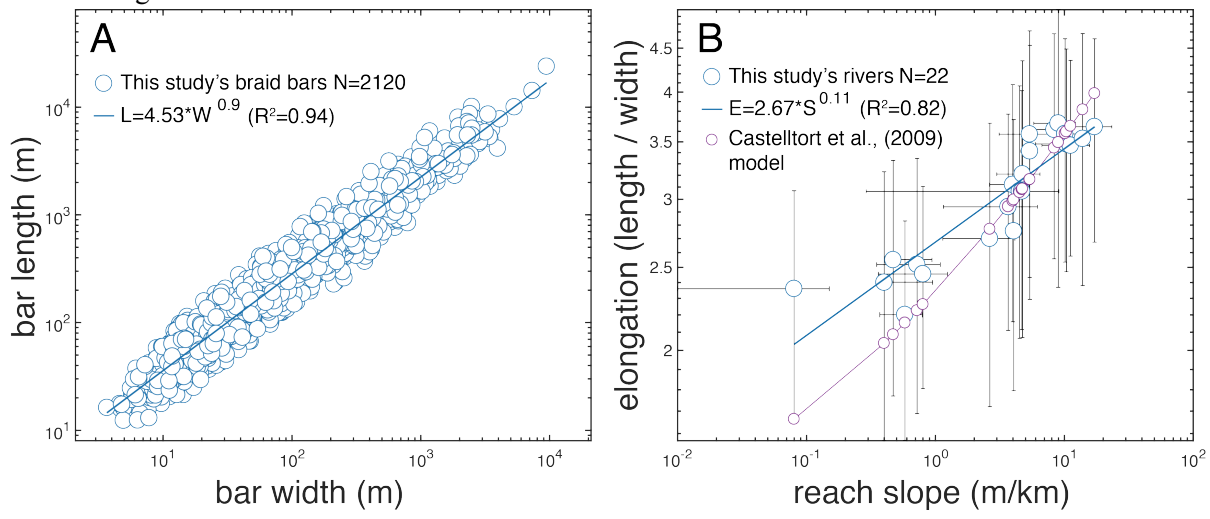

Figure 2 Braid bar scaling and relationship between bar elongation and slope. A) Length versus width of all measured bars (N=2120) in logarithmic space. Bar length scales non-linearly (exponent of 0.9) with bar width (see text). B) River

data of this study (blue circles) reveal an exponential relationship between mean bar elongation and river slope. This relation is close to the slope to channel convergence angle model (purple) of Castelltort et al (2009).

Fig 2B shows that mean bar elongation E of the studied rivers are positively correlated with their gradient S, yielding the following empirical relationship between bar elongation and river slope:

$$E = 2.67 \times S^{0.11}, R^2 = 0.82 \qquad \text{equation 3}$$

This trend line is, within the range given by standard deviation of elongation, similar to elongation predicted according to Castelltort et al (2009)'s model (equation 1). However, measurements deviate from prediction towards higher elongation at low slopes, and lower elongation at larger slopes.

4. Discussion

The lower than 1 exponent (0.9) found here in the scaling relationship between river bar length and width is also lower than Kelly (2006)'s exponent of 0.97 from an analysis of 1400 braid bars and indicates that braid bars become less elongated with increasing scale, i.e. as they become larger. This suggests, assuming that our data are representative of a broad spectrum of braided rivers, that bar geometry is not generally scale invariant (e.g., Sapozhnikov and Foufoula-Georgiou, 1996, Walsh and Hicks, 2002, Sambrook-Smith et al., 2005, and Kelly, 2006). Our results are instead more consistent with the suggestion by Hundey and Ashmore (2009), based on flume experiments, that confluence-bifurcation units constitute a "basic length scale of braided channel morphology".

The finding that braid bar elongation is both negatively correlated with scale (fig. 2A) and positively correlated with slope (fig. 2B) as expressed in equations (2) and (3) is consistent with known river slope-scaling relationships according to which river gradient decreases with scale (e.g., Hack, 1957). Such scale-dependence of slope in alluvial rivers is classically explained from the perspective of equilibrium channel gradient theory predicting that slope decreases with increasing drainage area (and thus with length, channel width, and macroform dimensions that all scale together with different exponent, e.g. Knighton, 1998, Kelly, 2006) and decreasing grain size in order to maintain constant transport capacity (e.g., Lane, 1937, Hack, 1957, see review in Sinha and Parker, 1996) at equilibrium. The negative slope-area relationship has also been explained as a result of the natural convergence of flow to areas of lower slopes, which thus accumulate the greatest drainage areas, even in the absence of erosion and sediment transport/deposition processes (e.g., Schorghofer and Rothman, 2002).

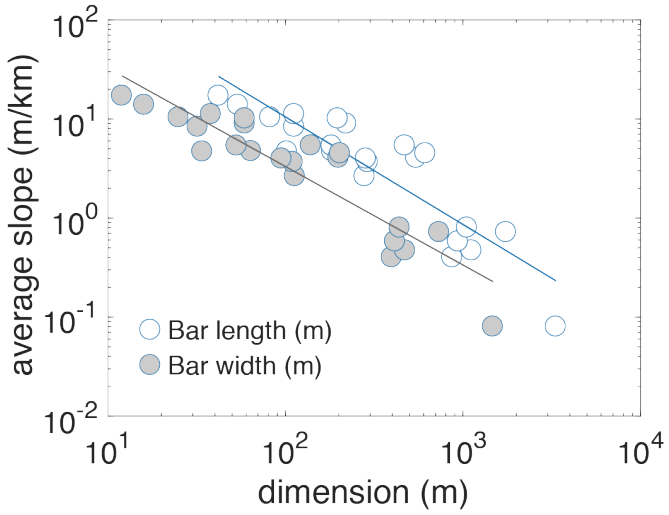

Figure 3 Scaling relationship between average river slope and mean bar width and length. Linear regression in logarithmic space yields R2 coefficients of 0.85 (grey dots, grey line) and 0.80 (white dot, blue line) for slope vs width and slope vs length relationships respectively.

Figure 3 confirms that the slope of rivers measured here decreases linearly with increasing scale as embodied in braid bar width, yielding (grey regression line on figure 3):

$$S = 322.48 \times W^{-0.99}, R^2 = 0.85 \qquad \text{equation 4}$$

A similar result is obtained by regressing reach slope with respect to braid bar length (blue regression line on figure 3):

$$S = 1560.49 \times L^{-1.09}, R^2 = 0.80 \qquad \text{equation 5}$$

In summary, short rivers in the studied database are steeper and display more elongated braid bars than larger rivers with shallower slopes and broader braid bars.

The offset and deviation in trend between predicted elongation (Fig. 2B, equation 1) and the elongation of bars as measured in this study probably reflects a number of processes that differ and/or play different roles in shaping drainage networks and braid bars, but the overall similarity of trend and absolute values nevertheless supports a commonality of processes underlying both types of systems. This is consistent with Murray and Paola (1994, 1997)'s findings from a series of numerical experiments with a cellular model of sediment transport, which suggested that braided and dendritic systems belonged to a continuum of landforms since they could successfully be simulated with the same set of sediment transport rules.

Example application

Recently, the development of 3D seismic technologies has allowed accurate documentation of planview morphology of sedimentary systems in the subsurface (Davies, Posamentier, Wood and Cartwright, 2007, Ethridge and Schumm, 2007, Miall, 2002). The bar elongation versus river slope relationship found here may take advantage of such development and provide a useful approach for inverting the slope of fossil rivers in the subsurface. Published analysis of a subsurface braided system in North-East China (Zhang, et al., 2009, Zhang, et al., 2010) identified through seismic strata-slicing techniques (Zeng, et al., 1998) is used here as an illustration of a possible application of the slope-elongation relationship to the evaluation of paleoslope from subsurface braid bar characterization.

In the DaGang area of the Bohaiwan Basin (North-East China), Zhang et al. (2009, 2010) have applied technologies of 90° phasing (Zeng and Backus, 2005) and stratal slicing (Zeng, Backus, Barrow and Tyler, 1998, Zeng, et al., 1998) to Neogene subsurface units. Their study reveals macroforms interpreted as braid bars that provide an opportunity to apply the relationship between average bar morphology and slope (equation 3). Figure 4A shows the interpreted delineation of bars in the stratal slice of the DaGang area (Zhang et al., 2010). Clearly, the identification of bars is not unambiguous, but it here only serves for the purpose of illustration. The analysis of all the bars (N=29) shown on the stratal-slice of figure 4A yields an average bar elongation of 2.11±0.61 (1σ). When all bars in contact with the borders of the slice and the possibly composite bars (large forms outlined around smaller forms on figure 4A) are removed (N=14), the average elongation is 2.40±0.71 (1σ). On the basis of these data, application of equation 3 (figure 4B) suggests that the DaGang braided river shown on figure 4 had a slope of 0.3794 m/km within a standard error range of [0.3124,0.4588].

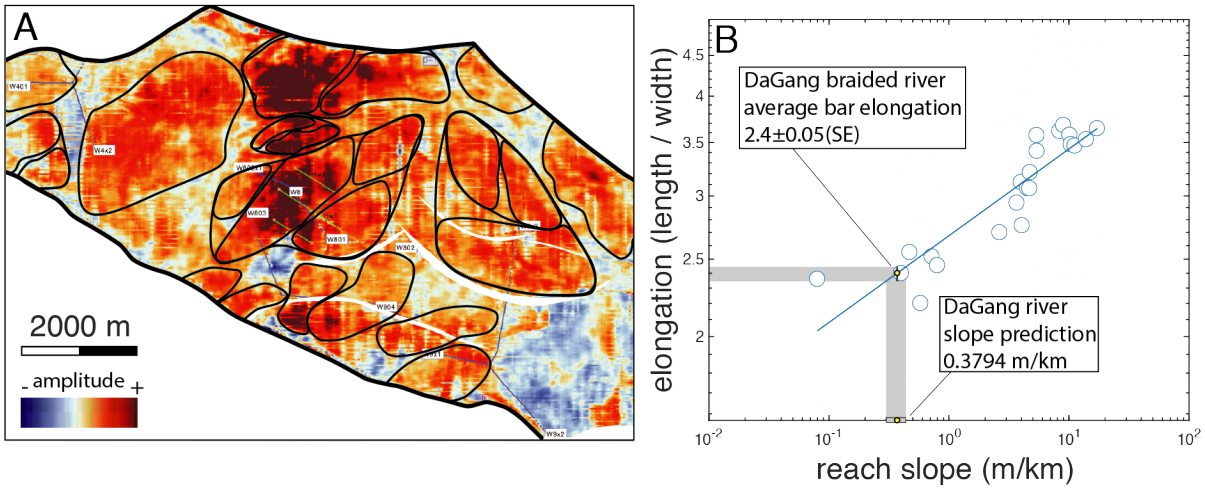

Figure 4 A) DaGang river interpreted subsurface morphology, with delineation of possible bar forms by Zhang et al (2010). B) Using the relationship between mean bar elongation and slope of modern systems (blue dots and blue line), a prediction of 0.3794 m/km paleoslope can be proposed for the DaGang river based on its mean elongation of 2.4±0.05 (Standard Error).

With data on channel depth and width, such paleoslope estimate can be used to reconstruct water discharge during channel-forming events and associated paleo-precipitation, which can be useful to infer climatic regimes and be integrated into more general facies models to inform predictions of sediment supply, reservoir properties and upstream/downstream trends in stratigraphic architecture. In the present case study, the obtained paleoslope constraints are plotted on a global database of slope and median grain size (D_{50}) data of modern rivers (Fig. 5A, Church and Rood, 1983, Van den Berg, 1995) in order to predict grain size from the subsurface. According to figure 5A and given our paleoslope estimates, the studied DaGang river deposits could be composed of either fine sand with $0.1mm \leq D_{50} \leq 1mm$ or gravel with $5mm \leq D_{50} \leq 100mm$. However, the distribution of slope is different within each grain size cluster of figure 5A: kernel probability density estimate (figure 5B) of slope for rivers with grain size of less than 1 mm is maximum for a slope of 0.30 m/km, whereas rivers with grain size greater than 10 mm have a most probable slope of 4.2 m/km (figure 5B). Thus, given the paleoslope estimate of 0.37 m/km for the DaGang area, it is more likely that the DaGang river had a bed made of fine sand with $0.1mm \leq D_{50} \leq 1mm$ rather than gravel. This hypothesis seems also to be consistent with grain size data from within an isochronous formation in an adjacent depobelt (Chen, 2007), which indicate median grain sizes of 1 mm and less. This would need additional independent constraints to be confirmed, but this is beyond the scope of the present paper.

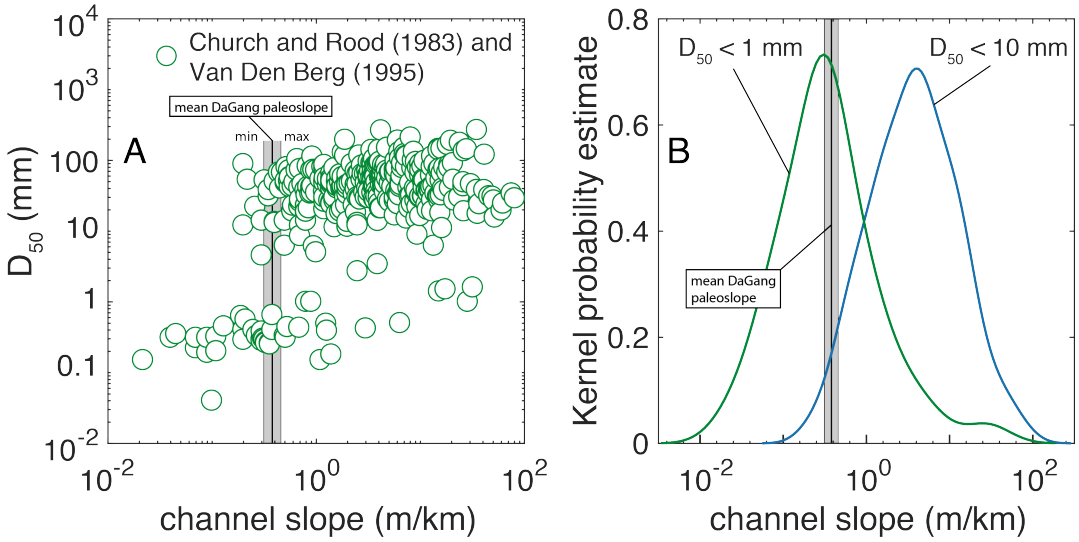

Figure 5 A) Grain size versus river slope data compilation from Church and Rood (1983) and Van Den Berg (1995). Plotting the mean paleoslope of the DaGang river and its range on this diagram allows a prediction of grain size from the subsurface. In the present case, for slopes of less than 1m/km but more than 0.1m/km (as predicted from the shape of braid bars in the DaGang area) two possible predictions arise because of the clustering of modern data in two distinct fields of sand (lower cluster) and gravel (upper cluster). B) Kernel probability density estimate of slope for median grain size less than 1 mm and greater than 10 mm for modern rivers. Paleoslope estimates of the DaGang river have a greater likelihood to belong to a river with grain size of less than 1 mm. This prediction is also favored based on observations in a nearby isochronous formation but more data would be required to test this hypothesis further.

Limitations

The approach presented here has several limitations. Predictions of paleoslope from braid bar elongation as seen from the subsurface shall be taken as order of magnitude estimates considering (1) the large spread of elongation data around average values in the modern examples, and (2) the fact that some geometrical change may take place during burial and preservation of bar morphology that may hinder direct comparison of ancient and recent braided systems (Sambrook Smith, et al., 2009). Another important drawback is the difficulty to ascertain the actual pattern (braided, meandering, anabranched) of the seismically imaged fluvial system. With these limitations in mind, the proposed approach provides, from subsurface information alone, a first-order estimate of the paleoslope and grain size of potential value to exploration, and which can be compared with other independent information to produce narrower predictions. In addition, this study provides a quantitative estimate of the braided river environment (in this case: low gradient, fine grained) that can be integrated in more general facies models and thus be potentially useful for the prediction of reservoir properties as well as downstream/upstream stratigraphic architecture. This finding complements other methods already developed for assessing paleoslope of ancient fluvial systems (e.g., Paola and Mohrig, 1996). With additional data on bankfull channel height collected from high-resolution seismic profiles through channel-overbank sections, paleoslope estimates from other methods more adequate for 2D data, could for instance be used with fig. 2B and fig 3 in combination with the Trampush et al (2014) empirical fit to produce tighter constraints on median grain size, but also simply to generate predictions of braid bars shape and scale of the river system. Finally, future addition of bar elongation versus river slope data will be needed to improve the relationship found here, as well as physical and numerical experiments, which could test it straightforwardly.

5. Conclusion

The analysis of the shape of bars in 22 modern braided rivers yields a positive relationship between bar elongation (length/width ratio) and river slope. Braid bars are more elongate in steep streams and broader in gently dipping rivers. This effect is attributed here to a possible topographic control on flow

directions of a similar nature as the topographic control on incipient drainage basin form, and thus emphasizes the potential importance of erosional processes in the braiding phenomenon.
The relationship can be useful for analyzing fossil braided systems from 3D-seismic data. In the example of the DaGang river succession, the analysis of bars identified on a seimic stratal-slice yields a slope of 0.3794 m/km within a standard error range of [0.3124,0.4588]. Using empirical data on grain size and river slope, this predicts a most likely median grain size of less between 0.1 mm and 1 mm, consistent with grain size data in an adjacent isochronous belt. The bar elongation to river slope relationship provides an addition to existing paleoslope methods, and can be used to generate first-order predictions of grain size from subsurface data, of potential interest in exploration.

Acknowledgements

Gredig Gaudenz provided a preliminary analysis of 10 rivers as part of his MSc thesis at ETH-Zürich. Xianguo Zhang provided unpublished material and technical explanations on the local geology of the DaGang area.

References

Ashmore, P.E., 1982. Laboratory modelling of gravel braided stream morphology Earth Surface Processes and Landforms, 7, 201-225.
Ashmore, P.E., 1991. How do gravel-bed rivers braid? Canadian Journal of Earth Sciences, 28, 326-341.
Bhattacharya, J.P., and Tye, R.S., 2004, Searching for modern Ferron analogs and applications to subsurface interpretation, in Chidsey, T.C., Jr., Adams, R.D., and Morris, T.H., eds., Regional to Wellbore Analog for Fluvial–Deltaic Reservoir Modeling: The Ferron Sandstone: American Association of Petroleum Geologists, Studies in Geology 50, p. 39–57.
Blondeaux, P., and Seminara, G., 1985, A unified bar–bend theory of river meanders: Journal of Fluid Mechanics, v. 157, p. 449–470.
Bridge, J.S., 2003. Rivers and floodplains: forms, processes, and sedimentary record. Blackwell Science, Oxford, U.K.
Bridge, J.S. and Lunt, I.A., 2006. Depositional models of braided rivers. In: Braided Rivers: Process, Deposits, Ecology and Management (G.H. Sambrook-Smith, J.L. Best, C.S. Bristow and G.E. Petts, eds). International Association of Sedimentologists.
Bristow, C.S. and Best, J.L., 1993. Braided rivers: perspectives and problems. In: Braided rivers (J.L. Best and C.S. Bristow, eds). Geological Society of London, London.
Carter, D.C., 2003. 3-D seismic geomorphology: Insights into fluvial reservoir deposition and performance, Widuri field, Java Sean Am. Assoc. Petr. Geol. Bull., 87, 909-934.
Castelltort, S., and Van Den Driessche, J., 2003, How plausible are high-frequency sediment supply-driven cycles in the stratigraphic record?: Sedimentary Geology, v. 157, no. 1-2, p. 3–13, doi: 10.1016/S0037-0738(03)00066-6.
Castelltort, S., Simpson, G. and Darrioulat, A., 2009. Slope-control on the aspect ratio of river basins Terra Nova, 21, 265-270.
Castelltort, S., and Yamato, P., 2013, The influence of surface slope on the shape of river basins: Comparison between nature and numerical landscape simulations : Geomorphology, v. 192, no. C, 71–79, doi: 10.1016/j.geomorph.2013.03.022.
Chen, R., 2007. Analysis of Fluvial Facies Sequence Stratigraphy of Neogene in the North Slope of Chengning Uplift, Chengdu University of Technology.
Church, M. and Rood, K., 1983. Catalogue of Alluvial River Channel Regime Data(D.o.G. University of British Columbia, ed, Vancouver.
Dade, W.B. and Friend, P.F., 1998. Grain-size, Sediment-Transport Regime, and Channel Slope in Alluvial Rivers J. Geol., 106, 661-675.

Davies, R.J., Posamentier, H.W., Wood, L.J. and Cartwright, J.A., 2007. Seismic Geomorphology. Applications to Hydrocarbon Exploration and Production. In: Geological Society of London Special Publications. The Geological Society of London, London.

Duller, R.A., Whittaker, A.C., Swinehart, J.B., Armitage, J.J., Sinclair, H.D., Bair, A., and Allen, P.A., 2012, Abrupt landscape change post-6 Ma on the central Great Plains, USA: Geology, v. 40, no. 10, p. 871–874, doi: 10.1130/G32919.1.

Ethridge, F.G. and Schumm, S.A., 2007. Fluvial seismic geomorphology: a view from the surface. In: Seismic Geomorphology. Applications to Hydrocarbon Exploration and Production (R.J. Davies, H.W. Posamentier, L.J. Wood and J.A. Cartwright, eds). The Geological Society of London, London.

Ferguson, R.I., 1993. Understanding braiding processes in gravel-bed rivers: progress and unsolved problems. In: Braided Rivers (J.L. Best and C.S. Bristow, eds). Geological Society of London, London.

Germanoski, D., and S. A. Schumm, 1993. Changes in braided river morphology resulting from aggradation and degradation, J. Geol., 101, 451 – 466.

Jung, K., Niemann, J.D., and Huang, X., 2011, Geomorphology: Geomorphology, v. 132, no. 3-4, 260–271, doi: 10.1016/j.geomorph.2011.05.014.

Kelly, S., 2006. Scaling and hierarchy in braided rivers and their deposits: examples and implications for reservoir modelling. In: Braided Rivers: Process, Deposits, Ecology and Management (G.H. Sambrook Smith, J.L. Best, C.S. Bristow and P. G.E., eds). Blackwell.

Knighton, 1998. Fluvial Forms and Processes, Arnold, London.

Lane, E.W., 1957, A study of the shape of channels formed by natural streams flowing in erodible material: MRD sediment series; no. 9,, p. 1–140.

Latrubesse, E.M., 2008. Patterns of anabranching channels: The ultimate end-member adjustment of mega rivers Geomorphology, 101, 130-145.

Leopold, L.B. and Wolman, M.G., 1957. River Channel Patterns: Braided, Meandering and Straight US Geol. Surv. Prof. Pap., 282-B, 39-85.

McGuire, L.A., Pelletier, J.D., Gómez, J.A., and Nearing, M.A., 2013, Controls on the spacing and geometry of rill networks on hillslopes: Rain splash detachment, initial hillslope roughness, and the competition between fluvial and colluvial transport: Journal of Geophysical Research: Earth Surface, v. 118, no. 1, 241–256.

Miall, A.D., 2002. Architecture and sequence stratigraphy of Pleistocene fluvial systems in the Malay Basin, based on seismic time-slice analysis. Am. Assoc. Petr. Geol. Bull., 86, 1201-1216.

Murray, A.B. and Paola, C., 1994. A cellular model of braided rivers Nature, 371, 54-57.

Murray, A.B. and Paola, C., 1997. Properties of a cellular braided-stream model Earth Surface Processes and Landforms, 22, 1001-1025.

Paola, C. and Mohrig, D., 1996. Palaeohydraulics revisited: palaeslope estimation in coarse-grained braided rivers Basin Res., 8, 243-254.

Parker, G., 1976. On the cause and characteristic scales of meandering and braiding in rivers Journal of Fluid Mechanics Digital Archive, 76, 457-480.

Parker, G., 1978, Self-formed straight rivers with equilibrium banks and mobile bed. Part 2. The gravel river: Journal of Fluid Mechanics, v. 89, no. 1, p. 127–146.

Pelletier, J.D., 2003. Drainage basin evolution in the Rainfall Erosion Facility: Dependence on initial conditions Geomorphology, 53, 183-196.

Phillips, L.F. and Schumm, S.A., 1987. Effect of regional slope on drainage networks Geology, 15, 813-816.

Rodriguez, E., Morris, C.S., Belz, J.E., et al., 2005. An Assessment of the SRTM Topographic Products. In: Technical Report JPL D-31639. Jet Propulsion Laboratory, Pasadena, CA.

Roduit, N., accessed August 2007. JMicroVision: Image analysis toolbox for measuring and quantifying components of high-definition images. http://www.jmicrovision.com.

Romans, B.W., Castelltort, S., Covault, J.A., Fildani, A., and Walsh, J.P., 2016, Environmental signal propagation in sedimentary systems across timescales: Earth Science Reviews, v. 153, no. C, p. 7–29, doi: 10.1016/j.earscirev.2015.07.012.

Sambrook Smith, G.H., Ashworth, P.J., Best, J.L., et al., 2009. The Sedimentology and Alluvial Architecture of a Large Braid Bar, Rio Parana, Argentina Journal of Sedimentary Research, 79, 629-642.

Sambrook Smith, G.H., Ashworth, P.J., Best, J.L., et al., 2005. The morphology and facies of sandy braided rivers: some considerations of scale invariance. In: Fluvial Sedimentology VII (M.D. Blum, S.B. Marriott and S.F. Leclair, eds). Blackwell, Oxford.
Sapozhnikov, V. and Foufoula-Georgiou, E., 1996. Self-affinity in braided rivers Water Resour. Res., 32, 1429-1439.
Schorghofer, N., and Rothman, D.H., 2002, Acausal relations between topographic slope and drainage area: Geophysical Research Letters, v. 29, no. 13, p. 11–1–11–4, doi: 10.1029/2002GL015144.
Schumm, 1977. The Fluvial System. John Wiley & Sons, New York.
Schumm, S.A., 1956. Evolution of drainage systems and slopes in badlands at Perth Amboy, New Jersey Geol. Soc. Am. Bull., 67, 597-646.
Schumm, S.A. and Khan, H.R., 1972. Experimental study of channel patterns Geol. Soc. Am. Bull., 83, 1755-1770.
Schuurman, F., Marra, W.A., and Kleinhans, M.G., 2013, Physics-based modeling of large braided sand-bed rivers: Bar pattern formation, dynamics, and sensitivity: Journal of Geophysical Research: Earth Surface, v. 118, no. 4, p. 2509–2527, doi: 10.1002/2013JF002896.
Simpson, G.D.H. and Schlunegger, F., 2003. Topographic evolution and morphology of surfaces evolving in response to coupled fluvial and hillslope sediment transport J. Geophys. Res, 108, 2300.
Sinha, S.K., and Parker, G., 1996, Causes of Concavity in Longitudinal Profiles of Rivers: Water Resources Research, v. 32, no. 5, p. 1417–1428, doi: 10.1029/95WR03819.
Thorne, J.A. and Swift, D.J.P., 1991. Sedimentation on continental margins, II: application of the regime concept. In: Shelf Sand and Sandstone Bodies (D.J.P. Swift, G.F. Oertel, R.W. Tillman and J.A. Thorne, eds). International Association of Sedimentologists, London.
Trampush, S.M., Huzurbazar, S., and McElroy, B., 2014, Empirical assessment of theory for bankfull characteristics of alluvial channels: Water Resources Research, v. 50, no. 12, 9211–9220, doi: 10.1086/626637.
Van den Berg, J.H., 1995. Prediction of alluvial channel pattern of perennial rivers Geomorphology, 12, 259-279.
Walsh, J., and Hicks, D.M., 2002, Braided channels: Self-similar or self-affine?: Water Resources Research, v. 38, no. 6, p. 18–1–18–6, doi: 10.1029/2001WR000749.
Williams, R.D., Brasington, J., and Hicks, D.M., 2016, Numerical Modelling of Braided River Morphodynamics: Review and Future Challenges: Geography Compass, v. 10, no. 3, p. 102–127, doi: 10.1111/gec3.12260.
Zeng, H. and Backus, M.M., 2005. Interpretive advantages of 90[degree]-phase wavelets: Part 2 --- Seismic applications Geophysics, 70, C17-C24.
Zeng, H., Backus, M.M., Barrow, K.T. and Tyler, N., 1998. Stratal slicing, Part I: Realistic 3-D seismic model Geophysics, 63, 502-513.
Zeng, H., Henry, S.C. and Riola, J.P., 1998. Stratal slicing, Part II: Real 3-D seismic data Geophysics, 63, 514-522.
Zeng, H. and Hentz, T.F., 2004. High-frequency sequence stratigraphy from seismic sedimentology: applied to Miocene, Vermillon Block 50, Tiger Shoal area, offshore Louisiana Am. Assoc. Petr. Geol. Bull., 88, 153-174.
Zhang, X., Lin, C. and Dong, C., 2009. From Amplitude to Architecture of Braided Channel Bars: the Sedimentological Interpretation of Stratal Slices in a Shallow-sea Seismic Survey, DaGang. In: CPS/SEG International Geophysical Conference and Exposition, Beijing.
Zhang, X., Lin, C., and Zhang, T., 2010, Seismic sedimentology and its application in shallow sea area, gentle slope belt of Chengning uplift: Journal of Earth Science, v. 21, no. 4, p. 471–479.

Supplementary Material

File: RIVER_DATABASE.xlsx

The supplementary material contains an Excel table names "RIVER_DATABASE.xlsx" with all JMicrovision© measurements of bar geometry for all rivers (one sheet per river, e.g. "Feshie") and the descriptive statistics of length, width and elongation (e.g., "Feshie Stats").

File: Castelltort_SupplementaryImages1.pdf
This pdf file contains the GoogleEarth© images of 16 of the studied rivers, with the corresponding delineation of braid bars.

File: Castelltort_SupplementaryImages2.kml
This is a kml file of 6 of the rivers. Instructions on how to use this file are given in the README.txt file.

File: README.txt
This is a text file with instructions on how to use the kml file Castelltort_SupplementaryImages2.kml

River name and location	Studied reach boundary coordinates		Reach length (km)	Reach slope (m/km)	Theoretical Max slope uncertainty (m/km)	Elevation data source	Number of measured bars	Average Bar length (m)	Average Bar width (m)	Mean bar elongation (length/width)	Standard deviation elongation
	Upstream boundary	Downstream boundary									
Brahmaputra (India)	26°38'N/93°09'E	26°12'N/91°11'E	208.98	0.08	0.14	SRTM3	125	3335	1475	2.360	0.71
Yukon reach 2 (Alaska)	66°0.7'N/144°12.4'W	66°11.3'N/144°36.8'W	27.28	0.40	1.10	GTOPO30	94	870	397	2.400	0.83
Yukon reach 1 (Alaska)	65°45.3'N/144°1.2'W	66°0.7'N/144°12.4'W	32.02	0.47	0.94	H1K	94	1117	472	2.550	0.78
Son (India)	24°32.5'N/83°53'E	25°02'N/84°19'E	71.73	0.58	0.42	SRTM3	55	937	414	2.201	0.63
Amguema (Russian Federation)	67°48.9'N/177°58.1'W	68°05.1'N/177°36.3'W	40.46	0.72	0.74	GTOPO30	61	1748	734	2.518	0.83
Kosi (Nepal)	26°49.03'N/87°8.76'E	26°33'N/86°57'E	34.20	0.80	0.88	SRTM3	38	1053	440	2.455	0.65
Tagliamento reach 1 (Italy)	45°57'N/12°54'E	45°52.6'N/12°57.97'E	10.01	2.64	3.00	SRTM3	70	279	113	2.700	0.98
Tagliamento reach 2 (Italy)	46°8.3'N/12°56.6'E	46°5.1'N/12°55.7'E	5.97	3.67	5.03	SRTM3	86	291	110	2.940	0.83
Maipo (Chile)	33°43.09'S/71°0.73'W	33°41.8'S/71°07.5'W	11.11	3.98	2.70	SRTM3	55	284	95	3.120	0.96
Bonnet Plume (Canada)	65°39.7'N/134°56.1'W	65°53.8'N/134°56.9'W	28.60	4.05	1.05	GTOPO30	71	545	199	2.755	0.96
Wairau (New Zealand)	41°39.75'S/173°10.0'E	41°34.5'S/173°27.3'E	25.99	4.50	1.15	SRTM3	55	614	203	3.066	1.00
Kluane Proglacial (Canada)	60°46.3'N/138°12.7'W	60°45.5'N/138°9.3'W	3.41	4.69	8.80	GoogleEarth	280	102	34	3.065	0.95
Zeravshan (Uzbekistan)	39°36.1'N/67°11.9'E	39°38.8'N/67°7.0'E	8.62	4.73	3.48	GoogleEarth	206	183	64	3.210	1.14
Wrangell-St Elias Proglacial 2 (Canada)	61°17.2'N/139°37.2'W	61°20.2'N/139°41.1'W	6.63	5.38	4.52	GoogleEarth	84	182	53	3.573	1.14
Rakaia (New Zealand)	43°36'S/171°47'E	43°42.5'S/171°57.5'E	18.67	5.40	1.61	GTOPO30	163	470	139	3.414	1.12
Atuel (Argentina)	35°07.8'S/69°33.7'W	35°10.3'S/69°32.3'W	6.15	8.34	4.88	SRTM3	215	112	32	3.617	1.06
Mendoza (Argentina)	33°3.20'S/68°46.93'W	33°3.35'S/68°43.97'W	4.71	8.98	6.37	SRTM3	57	220	59	3.679	1.31
Wrangell-St Elias Proglacial 1 (Canada)	61°14.7'N/139°35.3'W	61°17.2'N/139°37.2'W	5.75	10.13	5.22	GoogleEarth	98	197	59	3.575	1.04
Feshie (Scotland)	57°4.9'N/3°54.4'W	57°6.6'N/3°53.7'W	3.42	10.38	8.77	SRTM4	62	82	25	3.480	1.01
Bléone (France)	44°8.2'N/6°16.7'E	44°7.8'N/6°14.4'E	3.35	11.18	8.96	GoogleEarth	47	112	38	3.466	0.89
Schwarzwasser (Switzerland)	46°47.2'N/7°24.3'E	46°50'N/7°23.1'E	7.54	13.89	3.98	GoogleEarth	53	54	16	3.530	1.15
Bès (France)	44°9'N/6°14.7'E	44°7.8'N/6°14.3'E	2.42	17.17	12.40	Googleearth	52	42	12	3.644	0.97